9-2010

Analysis of a Deflating Soap Bubble

David P. Jackson
Dickinson College

Sarah Sleyman

Recommended Citation

Jackson, David P., and Sarah Sleyman. "Analysis of a Deflating Soap Bubble." *American Journal of Physics* 78, no. 10 (2010): 990-994. https://aapt.scitation.org/doi/10.1119/1.3442800

Analysis of a deflating soap bubble

David P. Jackson and Sarah Sleyman
Department of Physics and Astronomy, Dickinson College, Carlisle, Pennsylvania 17013

(Received 7 January 2010; accepted 12 May 2010)

A soap bubble on the end of a cylindrical tube is seen to deflate as the higher pressure air inside the bubble escapes through a tube. We perform an experiment to measure the radius of the slowly deflating bubble and observe that the radius decreases to a minimum before quickly increasing. This behavior reflects the fact that the bubble ends up as a flat surface over the end of the tube. A theoretical analysis reproduces this behavior and compares favorably with the experimental data.
[DOI: 10.1119/1.3442800]

I. INTRODUCTION

Soap bubbles have long fascinated kids and adults alike. Most people have enjoyed at one time or another the beauty and splendor of a well formed soap bubble glistening in the sunlight. This beauty must have been evident to many 17th and 18th century artists who included bubbles in their paintings.[1] Some individuals have developed exquisite control over soap bubbles and can construct beautiful "sculptures," including such exotic shapes as tetrahedrons, cubes, octahedrons, and dodecahedrons.[2] Soap films have been used to demonstrate minimal surfaces, solutions to Laplace's equation, and many other mathematically interesting structures.[3] Beyond that, soap films have been studied in new and interesting ways, including the study of two-dimensional fluid dynamics,[4] soap films in electric fields,[5] and magnetic soap films.[6]

A collapsing spherical soap bubble is fairly straightforward to analyze and has been used to determine the surface tension of the soap film.[7] Although this type of experiment is a good project for introductory students, we describe here a similar but more sophisticated experiment that is appropriate for upper-division students. The main difference with previous studies is that the bubble is placed on a hollow tube with a relatively large radius. As a result, instead of the bubble radius decreasing monotonically to zero, the radius first decreases and then increases as the bubble flattens to cover the end of the tube. When carefully performed, the agreement between experiment and theory is very good, adding a "wow" factor that gives students a strong sense of accomplishment and a positive overall experience.

Depending on the amount of assistance provided, this project can take students from a week—if the experiment is already set up and students are provided with the theory to a semester—if the project is open-ended and students are expected to set up the equipment and derive all the equations on their own. In our case the project was open-ended so that the students were responsible for dealing with all the difficulties that inevitably arise when doing research.

II. EXPERIMENTAL DETAILS

The basic experiment is qualitatively very simple—a spherical soap bubble of radius $r(t)$ is blown on the end of a hollow cylindrical tube and videotaped as it deflates. As mentioned, the hollow tube has a relatively large radius R, which significantly alters the results compared to previous studies. In this configuration the bubble radius decreases and reaches a minimum when the bubble is a hemisphere with $r=R$. After this point, the radius increases without bound.

The experimental setup is shown in Fig. 1. A syringe is connected via flexible tubing (through a rubber stopper) to the bottom of a hollow cylindrical tube approximately 2.5 cm in diameter. We use a 50 ml glass syringe, but a plastic syringe should work just as well. The flexible tubing acts as the inflation tube and also connects to a precision manometer used to measure the pressure difference between the inside and outside of the bubble. Air escapes from the bubble through a small diameter deflation tube (radius $s \sim 1$ mm) inserted through the rubber stopper. The bubble can be held at a fixed radius by inserting a small plug on the end of the deflation tube; this is important when measuring the surface tension of the soap film as discussed in the following.

A. Preliminary details

As shown in Fig. 1, our setup has the bubble sitting on top of the tube rather than hanging from the bottom. This setup is chosen to prevent liquid from collecting on the bubble and causing it to deform. This orientation is stable for reasonably sized bubbles ($r \lesssim 5R$). Because the liquid will drain down the inside and outside of the tube, care must be taken to prevent the liquid from entering the inflation and deflation tubes by inserting these tubes all the way through the rubber stopper so that they protrude into the interior of the large diameter tube. Paper towels wrapped around the outside of the tube prevent the experiment from getting too messy.

Measuring the bubble radius as a function of time is accomplished by videotaping the deflating bubble and carefully analyzing the images. Because the deflation tube is so narrow, the entire deflation process can take several minutes even for a modest-sized bubble. Such a lengthy deflation time makes it essential that our soap solution produce long lasting bubbles. Numerous recipes for soap bubble solutions can be found on the web, and we experimented with many different types. Without going to heroic measures,[8] a good starting formula for producing long lasting bubbles is a mixture of (approximately) one part glycerine, one part water, and one part Dawn Ultra.[9] This solution remains satisfactory even when adding much more water.

To quantitatively compare the experimental data to a theoretical prediction, we need to know the surface tension of the soap film. The surface tension can be easily measured using the same apparatus.

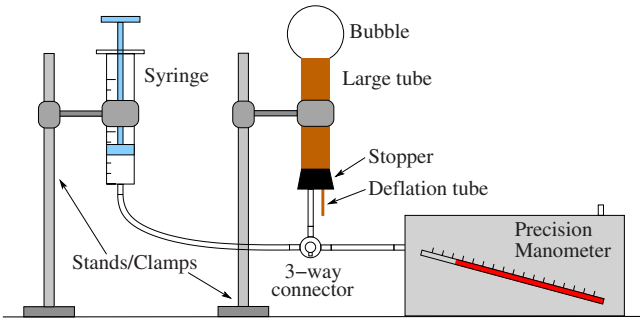

Fig. 1. A schematic diagram of the bubble deflation experiment. A syringe is used to inflate the bubble, and a precision manometer is used to measure the pressure difference between the interior and exterior of the bubble.

B. Measuring the surface tension

Measuring the surface tension of soap solutions using the apparatus shown in Fig. 1 has been discussed,[10] and we follow a similar procedure. The pressure difference of the gas across a spherical soap film is given by the Young–Laplace equation

$$\Delta P = P_{\text{in}} - P_{\text{out}} = \frac{4\sigma}{r}, \tag{1}$$

where σ is the surface tension of the soap film, P_{in} and P_{out} are the gas pressures inside and outside the bubble, and r is the radius of the bubble.

To determine the surface tension, we inflate a soap bubble and allow it to deflate in stages, plugging the deflation tube between each stage.[11] A high-resolution digital photograph is taken for a series of static bubble sizes. The manometer scale is included in each photograph so that both the pressure difference and the bubble radius can be determined from the image. Although finding the pressure difference is as simple as reading the manometer scale, determining the bubble radius is more difficult. We analyzed these images using the VISION ASSISTANT software program developed by National Instruments.[12] This program fits a circle to a user-defined annular region of interest. Such a tool is extremely useful when only a small portion of the circle is visible.

Figure 2 shows a plot of ΔP versus $4/r$ for a typical experiment; the linearity of the data is evident. The value of the surface tension obtained from the slope of the best-fit line is $\sigma = 0.0258$ N/m.

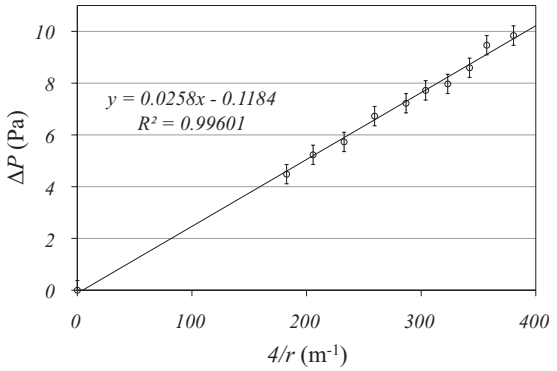

Fig. 2. Typical experimental data for determining the surface tension of a soap film. As shown in Eq. (1), the surface tension is given by the slope of the best fit line.

C. Laminar flow

Before discussing the actual bubble deflation experiment, we discuss the size of the deflation tube. Our theoretical analysis depends on the flow through the deflation tube being laminar. This flow can be verified experimentally by filling the soap bubble with smoke and watching the flow pattern emanate from the deflation tube. Alternatively, we can estimate the deflation tube radius by examining the Reynolds number Re. The latter is a dimensionless number that compares inertial to viscous forces for given fluid flow conditions. Laminar (smooth and stable) flow occurs at low Reynolds numbers when viscous forces are dominant, and turbulent (chaotic and unstable) flow occurs at large Reynolds numbers when inertial forces dominate.

Laminar flow through a tube is governed by Poiseuille's equation[13]

$$Q = \frac{\pi s^4}{8\eta}\frac{|\Delta P|}{L}, \tag{2}$$

where Q is the (volumetric) flow rate through the tube, η is the (dynamic) viscosity of the fluid, s and L are the radius and length of the tube, and ΔP is the pressure difference from one end of the tube to the other. To estimate the Reynolds number for flow through a pipe, we take ρv^2 as the inertial force and $\eta \nabla v \sim \eta v/(2s)$ as the viscous force, where ρ is the mass density and v is the characteristic velocity of the fluid. The Reynolds number for flow through a pipe is

$$\text{Re} \approx \frac{\rho v^2}{\eta v/(2s)} = \frac{2\rho Q}{\eta \pi s}, \tag{3}$$

where we have used $v = Q/(\pi s^2)$ as the characteristic velocity of the fluid. For a deflating bubble the pressure difference across the deflation tube is given by the Young–Laplace condition (1). Combining Eqs. (1)–(3) gives the radius of the deflation tube as a function of the Reynolds number as

$$s = \left(\frac{rL\eta^2\,\text{Re}}{\rho\sigma}\right)^{1/3}. \tag{4}$$

For fluid flow through a pipe, turbulent flow usually occurs for $\text{Re} > 4000$, while laminar flow occurs for $\text{Re} < 2300$; in between, either flow is possible.[13] Thus, to safely guarantee laminar flow, we require that the Reynolds number be less than 2000 for the entire deflation process. We use our measured value of the surface tension, a minimum bubble radius of 1 cm, a deflation tube length of 15 cm, and room temperature air properties. From Eq. (4) we find that the radius of the deflation tube must be less than ≈ 3 mm. Although this value is only an estimate, it demonstrates that the deflation tube must be relatively narrow. The real justification for assuming laminar flow comes from observing the flow using a smoke-filled bubble.

D. Bubble deflation

We measure the bubble radius as a function of time by using a standard video camera to record the deflation. Because pressure data are not needed for the deflation experiment, the camera is zoomed so that the bubble fills the entire screen. Commercial video cameras take data at 30 frames/s, and we need to analyze only a small portion of the resulting video frames to obtain a reasonable set of data. As mentioned, determining the radius of the bubble is not trivial,

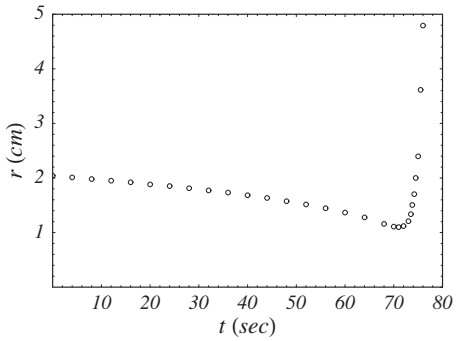

Fig. 3. Raw data for a deflating soap bubble. A slow decrease in the bubble's radius is followed by a rapid increase.

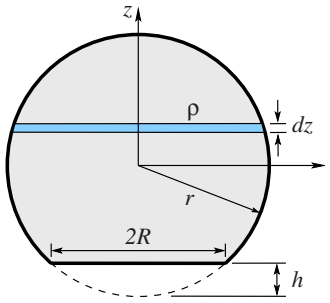

Fig. 4. A partial sphere results when a plane cuts through a sphere of radius r leaving a flat circular face of (fixed) radius R. The volume of such a partial sphere is found by integrating slices of thickness dz along the z-axis.

particularly when the bubble radius has begun increasing. A good image analysis program is essential to obtain accurate data. Figure 3 shows a typical set of raw data. The data behave as expected: A slowly decreasing bubble radius followed by a rapid increase.

III. THEORETICAL ANALYSIS

The theoretical analysis is complicated by the fact that the deflating bubble is not a perfect sphere. Where the bubble intersects with the large tube, the bottom of the sphere is cut off, leaving only a partial sphere. Because the analysis proceeds along the same lines in either case, it is instructive to first analyze the much simpler case of a deflating full sphere.

A. Full sphere

If a full sphere deflates through a tube such that the flow is laminar, the pressure difference is given by Eq. (1), and the (volume) flow rate is given by Eq. (2). We combine Eqs. (1) and (2) to find the volumetric flow rate out of the sphere

$$Q = \frac{\pi s^4 \sigma}{2\eta L r} = -\frac{dV_s}{dr}\frac{dr}{dt}, \tag{5}$$

where V_s is the volume of a sphere. The minus sign arises because Q is a positive quantity and the change in volume of a deflating sphere is negative. Equation (5) is a separable differential equation, which is solved by integrating

$$\left(r\frac{dV_s}{dr}\right)dr = -\frac{\pi s^4 \sigma}{2\eta L}dt. \tag{6}$$

We let $V_s = 4\pi r^3/3$ and integrate both sides of Eq. (6) to yield

$$r(t) = r_0\left[1 - \frac{\sigma s^4 t}{2\eta L r_0^4}\right]^{1/4}, \tag{7}$$

where r_0 is the radius of the bubble at $t=0$. As is often the case, it is convenient to rewrite the solution in terms of dimensionless variables. We define $\tilde{r} \equiv r/r_0$, $\tilde{s} \equiv s/r_0$, and $\tilde{t} \equiv t/\tau$, where $\tau \equiv 2\eta L/(\sigma \tilde{s}^4)$, and see that

$$\tilde{r}(\tilde{t}) = (1 - \tilde{t})^{1/4}. \tag{8}$$

One advantage of the dimensionless formulation is that any combination of the parameters σ, s, η, L, and r_0 produces the same graph, which makes it convenient to compare multiple experiments performed with different parameters. According to Eq. (8), $\tilde{r}$ drops to zero at $\tilde{t}=1$, or when $t=\tau$. This collapse time has been used to estimate the surface tension of a soap film.[7,14] To put it another way, τ represents a characteristic time for a spherical bubble to go from $r=r_0$ to $r=0$ when the escaping air flows through a tube of length L and radius s according to Poiseuille's law. Note that τ is proportional to r_0 to the fourth power. Thus, if we double the initial radius, the bubble will take 16 times longer to deflate. This important information would be missed if we looked only at a graph of Eq. (8). When using dimensionless variables, it is important to think physically about what they actually mean.

B. Partial sphere

Although the analysis for a full sphere is straightforward, it breaks down as the radius of the sphere approaches the radius of the deflation tube. At this point, Eq. (7) ceases to be valid. To find an equation valid for all times, we repeat the analysis and replace the volume of a full sphere with that of a partial sphere V_{ps}.

The main difficulty is finding the volume of a partial sphere. This quantity is straightforward to calculate in terms of the quantity h (see Fig. 4). We take advantage of the cylindrical symmetry and integrate horizontally sliced volume elements $dV = \pi\rho^2 dz$ along the z-axis. Here, ρ is the distance from the z-axis to the surface of the sphere. Carrying out the integration gives

$$V_{ps} = \int_{h-r}^{r} \pi\rho^2 dz = \int_{h-r}^{r} \pi(r^2 - z^2)dz \tag{9a}$$

$$= \tfrac{2}{3}\pi r^3 - \pi(h-r)\left[r^2 - \tfrac{1}{3}(h-r)^2\right]. \tag{9b}$$

Equation (9b) holds for any sized partial sphere, from a full sphere ($h \to 0$) to a flat surface ($h \to 2r$).

We would like to simply substitute V_{ps} for V_s in Eq. (6). But first we must eliminate h from Eq. (9b) and express V_{ps} solely in terms of r. To do so, we make use of the constraint imposed by the large diameter tube (see Fig. 4) and write $(h-r) = \mp\sqrt{r^2 - R^2}$, where the upper (lower) sign corresponds to a bubble that is larger (smaller) than a hemisphere. Substitution into Eq. (9b) gives

$$V_{ps} = \frac{\pi}{3}[2r^3 \pm (2r^2 + R^2)\sqrt{r^2 - R^2}]. \tag{10}$$

Although a bit tedious, replacing V_s with V_{ps} in Eq. (6) leads to an integrable equation. In this case, it is convenient

to first make the equation dimensionless by scaling all lengths by R instead of r_0 as we did in the full sphere case. The resulting equation is integrated to give

$$\tilde{t}_{\pm}(\tilde{r}) = I_{+}(\tilde{r}_0) - I_{\pm}(\tilde{r}), \tag{11}$$

where

$$4I_{\pm}(x) \equiv 2x^4 \pm [(2x^2+1)x\sqrt{x^2-1} + \ln(x+\sqrt{x^2-1})], \tag{12}$$

and $\tilde{t} \equiv t/\tau$ with the characteristic time given by $\tau \equiv 2\eta L/(\sigma s^4)$. In this case it is important to realize that s has been scaled by R instead of r_0. Thus, the characteristic time tells us how long it takes a (full) spherical bubble of initial radius R to deflate through a tube of length L and radius s. In Eq. (11), $\tilde{t}_{+}(\tilde{r})$ is used when the bubble is larger than a hemisphere and $\tilde{t}_{-}(\tilde{r})$ is used when the bubble is smaller than a hemisphere. Although Eqs. (11) and (12) cannot be inverted analytically to yield $\tilde{r}(\tilde{t})$, it is simple to splice $\tilde{t}_{+}$ and $\tilde{t}_{-}$ together and plot $\tilde{t}$ as a function of $\tilde{r}$.

To compare theory to experiment, we first need to rescale the experimental data. It is not obvious what value to use for R—the inner radius, the outer radius, the average, or something else? By looking carefully at the images from the experiment, it appears that the bubble is "pinned" to the outer radius when it is larger than a hemisphere and then becomes pinned to the inner radius when it is smaller than a hemisphere. Thus, it might seem like the average radius would be a good choice to use. However, during the deflation process, the bubble is mostly larger than a hemisphere and spends little time smaller than a hemisphere, making it reasonable to choose a value halfway between the average and the outer radius ($R=1.093$ cm). As it happens, it matters little which value we use for R.

In addition to R, we need a number of other values to rescale the time. We measure all these values except the viscosity, which is found using the gas viscosity calculator.[15] We find $L=15.1$ cm, $\sigma=0.0258$ N/m (from Fig. 2), $r_0=2.04$ cm, and $s=0.165(\pm 0.01)$ cm and use $\eta=1.837\times 10^{-5}$ N s/m^2. Unfortunately, if these values are used as is, the fit is not very good. The problem is that τ depends on s/R to the fourth power and is extremely sensitive to small changes in either of these two parameters. Because s is the least accurate of our measured values, we treat everything else as fixed and adjust s to obtain a good fit to the data. (This procedure is why choosing a slightly different value for R does not really matter.)

Figure 5 shows the partial sphere prediction using Eqs. (11) and (12) after fine-tuning s for the best fit; we find $s=0.1688$ cm, well within the measured uncertainty. (Because the results depend so sensitively on s, four decimal places of accuracy must be used to obtain such a good fit.) The agreement with experiment is impressive and is exciting for students. For comparison purposes, we also plot the full sphere prediction using an appropriately scaled version of Eq. (7) for the same value of s.[16] Note that the full sphere prediction is indistinguishable from the partial sphere prediction until the bubble radius is within $\approx 20\%$ of the tube radius, at which point the two models diverge.

A quick glance at Fig. 5 suggests that a partial sphere will collapse in approximately the same amount of time as a full sphere. In fact, a partial sphere takes infinitely long to complete its deflation, as can be verified by approximating $\tilde{t}$ for large $\tilde{r}$: $\tilde{t}_{-}(\tilde{r}\to\infty) \approx \frac{1}{4}\ln(2\tilde{r})$. Because of this logarithmic dependence, the concept of a "collapse" time for a partial sphere is not well defined. The concept of a collapse time for a full sphere is also suspect because any deflating sphere must be connected to a deflation tube of some sort. To be truly accurate, the collapse time should be defined as the time it takes a bubble to go from an initial radius to some final (nonzero) radius. As long as the final radius is moderately larger than the deflation tube radius, such a collapse time will be nearly indistinguishable between the full sphere and partial sphere models.

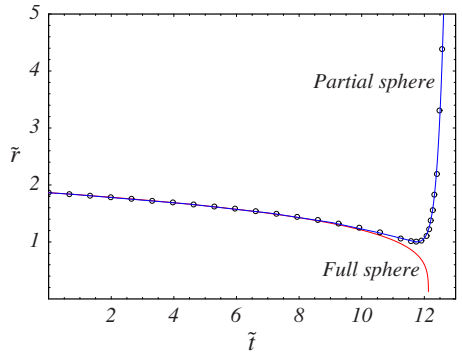

Fig. 5. The partial sphere model of Eq. (11) and an appropriately dimensionless version of the full sphere model of Eq. (7) are compared to the experimental data.

IV. CONCLUSION

We have described a soap bubble deflation experiment that makes a wonderful undergraduate project. This project has strong experimental and theoretical components that can be understood by physics majors, yet is challenging enough to maintain the interest of the brightest students. The basic experiment is fairly straightforward with the exception of the precision manometer, which might be unfamiliar to students. A manometer can be purchased for less than $100, and students should not have much difficulty getting it working. The most difficult part of the experiment is analyzing the images. A good image analysis program is critically important. Students will likely have much more difficulty with the theoretical analysis, which can be overwhelming if not handled carefully. Breaking down the analysis into small pieces and assigning them one at a time are essential to helping students make timely progress.

If appropriate care is taken to analyze the data, the results (as displayed in Fig. 5) are impressive enough to make students feel like the project was a success. Because it is possible for students to become frustrated before everything comes together, it is essential for the faculty advisor to provide appropriate guidance, particularly during the more challenging phases of the project. Nevertheless, we believe that this type of open-ended project provides a valuable learning experience for undergraduate majors, and we encourage others to incorporate such project-based learning into the physics curriculum.

ACKNOWLEDGMENTS

We gratefully acknowledge Derek Moulton for helpful advice regarding this project and Thomas Schenck and Jacob Heberling for assisting with the experiments.

[1] F. Behroozi, "Soap bubbles in paintings: Art and science," Am. J. Phys. **76**, 1087–1091 (2008).
[2] For those interested in seeing some fantastic soap bubble creations, two great websites are ⟨www.tomnoddy.com⟩ and ⟨www.soapbubble.dk.en⟩.
[3] An excellent introduction to the scientific aspects of soap bubbles can be found in Cyril Isenberg, *The Science of Soap Films and Soap Bubbles* (Dover, New York, 1992).
[4] M. A. Rutgers, X. L. Wu, and W. B. Daniel, "Conducting fluid dynamics experiments with vertically falling soap films," Rev. Sci. Instrum. **72**, 3025–3037 (2001).
[5] D. E. Moulton and J. A. Pelesko, "Theory and experiment for soap-film bridge in an electric field," J. Colloid Interface Sci. **322**, 252–262 (2008).
[6] D. E. Moulton and J. Lega, "Reverse draining of a magnetic soap film—Analysis and simulation of a thin film equation with non-uniform forcing," Physica D **238**, 2153–2165 (2009).
[7] Gören Rämme, "Surface tension from deflating a soap bubble," Phys. Educ. **32**, 191–194 (1997).
[8] A complicated recipe (from a physicist's perspective) for very long-lived soap bubbles is given by A. L. Kuehner, "Long-lived soap bubbles," J. Chem. Educ. **35**, 337–338 (1958).
[9] Although it would seem that the precise detergent is unimportant, we found Dawn Ultra to perform significantly better than other detergents.
[10] F. L. Román, J. Faro, and S. Velasco, "A simple experiment for measuring the surface tension of soap solutions," Am. J. Phys. **69**, 920–921 (2001).
[11] We use a paper towel soaked in soap solution and rub it across the top of the tube to prep the system for bubble blowing.
[12] National Instruments equipment and software can be found at ⟨www.ni.com⟩.
[13] See, for example, T. E. Faber, *Fluid Dynamics for Physicists* (Cambridge U. P., Cambridge, 1995).
[14] L. Sibaiya, "Time of collapse of a soap bubble," Nature (London) **3784**, 527–527 (1942).
[15] A simple-to-use online gas viscosity calculator can be found at ⟨www.lmnoeng.com/Flow/GasViscosity.htm⟩.
[16] As expected, the fourth-power dependence on s/R causes a full sphere with $\tilde{r}_0=1.866$ to take $(1.866)^4 \approx 12.1$ times longer to deflate than a full sphere with $\tilde{r}_0=1$ (which collapses at $\tilde{t}=1$).

Selenium Cell. The resistivity of thin layers of selenium is a function of the intensity of the illumination falling on the surface of the material. This property enabled it to be used as the detector for an optical communication system developed by Alexander Graham Bell in 1879-80. The first selenium cell, designed by Siemens in 1876, was made by winding two thin platinum wires around a sheet of mica, and then covering the surface with a thin film of molten selenium. The large surface-to-volume ratio was necessary because photoconductivity is a surface effect, while the resistivity of the selenium is quite high. This example is in the Greenslade Collection, and was sold by Max Kohl of Chemnitz, Germany about 1900 for $10.00. (Photograph and Notes by Thomas B. Greenslade, Jr., Kenyon College)